

Low temperature thermal properties of mesoscopic normal-metal/superconductor heterostructures

D. A. Dikin, S. Jung and V. Chandrasekhar

Department of Physics and Astronomy, Northwestern University, Evanston, IL 60208, USA

Although the electrical transport properties of mesoscopic metallic samples have been investigated extensively over the past two decades, the thermal properties have received far less attention. This may be due in part to the difficulty of performing thermal measurements on sub-micron scale samples. We report here quantitative measurements of the thermal conductance and thermopower of a hybrid normal-metal/superconductor heterostructure, which are made possible by the recent development of a local-thermometry technique. As with electrical transport measurements, these thermal measurements reveal signatures of the phase coherent nature of electron transport in these devices.

As the packing density of electronic devices on a single chip continues to increase, the issue of heat transport and dissipation in nanometer scale structures becomes of increasing importance. Although many experiments have focused on the electrical properties of micro- and nanometer scale structures, the thermal characteristics of such devices are only beginning to be explored. In addition to addressing critical issues related to the fabrication of the next generation of electronic devices, exploration of the thermal properties of such mesoscopic structures may also lead to the discovery of new phenomena, particularly when the quantum phase coherence length of the thermal carriers is comparable to the sample dimensions.

The difficulty in making measurements of thermal properties on mesoscopic devices stems from the problem of accurately measuring the temperature on such a small size scale, without disturbing the device being measured. Although numerical estimates of thermal properties of mesoscopic samples may be obtained by modeling the heat flow, quantitative measurements have only recently become possible. Recently, in a beautiful experiment, Schwab et al.¹ were able to measure the quantization of heat conduction in a ballistic phonon waveguide using sophisticated lithographic and measurement techniques. However, equivalent measurements of the thermal properties associated with electronic conduction in mesoscopic metallic samples have not been reported. In this Communication, we describe our quantitative measurements of the electronic thermoelectric power and the thermal conductance of single, doubly-connected, micron-size heterostructures formed from a superconductor and a normal metal, using local thermometry techniques that we recently developed². Although the thermal conductance shows no dependence on magnetic field to within our measurement sensitivity, the thermopower shows oscillations as a function of magnetic field, demonstrating the phase coherent nature of thermal transport in this regime.

The electrical current I and thermal current I^T through a metallic sample are related to the voltage difference ΔV and the temperature difference ΔT by the

transport equations³:

$$I = G\Delta V + \eta\Delta T \quad (1)$$

and

$$I^T = \zeta\Delta V + \kappa\Delta T \quad (2)$$

Conceptually at least, thermal measurements on metallic samples are relatively straightforward. A temperature differential ΔT is applied to the sample, and the voltage ΔV across the sample is measured, under the condition that the current I through the sample is 0. The resulting ratio $S = \Delta V/\Delta T = \eta/G$ is called the thermopower. The ratio $G^T = I^T/\Delta T$ measured under the same conditions is the thermal conductance. Replacing $\Delta V = S\Delta T$ from Eq. (1) into Eq. (2), one obtains $G^T = S\zeta + \kappa$. For typical metals, the first term in this expression is much smaller than the second one, so that G^T can be approximated by $G^T \approx \kappa$.

In order to obtain quantitative measurements of the thermal conductance and thermopower on mesoscopic samples, one needs to accurately measure the local electron temperature on submicron length scales. The requirement of any electron thermometer on this size scale is that it should not disturb the local electron gas appreciably, while still remaining sensitive to changes in the temperature. Recently, the Saclay group has demonstrated in a series of beautiful experiments the possibility of using normal-metal/insulator/superconductor (NIS) tunneling spectroscopy to probe the local electron distribution in a mesoscopic normal-metal sample⁴. While these thermometers can accurately measure the electron temperature on the size scale of approximately one hundred nanometers, the difficulty of fabricating the tunnel junctions (usually done by *in situ* shadow evaporation techniques) precludes using this technique on more complex sample geometries. In addition, determination of the temperature requires measuring a full dc current voltage characteristic at each point, and then fitting the measured curve in order to obtain the temperature, making it time-consuming to use when many data points are

to be obtained. An alternative technique that we have developed² is to use the strong temperature dependence arising from the superconducting proximity effect in a normal metal⁵ as a local electron temperature thermometer. As we demonstrate below, the thermometers are relatively simple to fabricate and measure, and provide the ability to measure the local electron temperature at essentially any point on a complex mesoscopic sample.

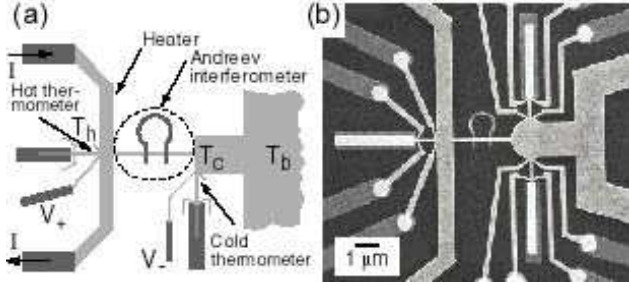


FIG. 1. (a) Schematic of our sample design for measuring the thermal properties of a mesoscopic NS structure, an Andreev interferometer. Dark gray is superconductor, lighter area is normal metal. The Andreev interferometer is encircled by a dotted line. (b) Scanning electron micrograph of one of our actual devices fabricated by conventional electron-beam lithography techniques. Dark gray areas are superconductor (Al), while the lighter areas are normal metal (Au). For thermopower measurements, the thermal voltage is measured using the contacts labeled V_+ and V_- , as seen in (a).

Figure 1 shows a schematic and a scanning electron micrograph of one of the devices we have measured. Three such samples were measured, although the results of only one are presented here. The devices were fabricated by conventional multi-level electron-beam lithography technique on oxidized Si substrates. The 65 nm thick Au wires and contacts were patterned and evaporated first, after which the 65 nm thick Al film was evaporated following O_2 plasma etching to ensure good interfaces between the Au and Al films. From weak localization measurements⁶ on long Au wires with similar properties, we determined the electron phase coherence length to be $L_\phi \cong 3.5 \mu\text{m}$ at $T = 300 \text{ mK}$, and the diffusion constant in the Au to be $D \cong 1.9 \times 10^{-2} \text{ m}^2/\text{sec}$, resulting in a superconducting coherence length in the normal metal $L_T \cong 0.38 \mu\text{m}$ at $T=1 \text{ K}$.

The sample itself is a so-called Andreev interferometer⁷, and consists of a normal metal Au wire ($2.44 \mu\text{m}$ long and $0.12 \mu\text{m}$ wide) interrupted in the middle by a superconductor (Al) to form a loop. Similar Andreev interferometers have been recently shown to exhibit a number of interesting properties; in particular, the resistance⁸ and thermopower⁹ show periodic oscillations as a function of magnetic field, with a fundamental period corresponding to a superconducting flux quantum $h/2e$ through the area of the loop. The thermometers on either end of the Andreev interferometer consist of single Au wires with four probes connected to Al leads. A

superconducting film placed close to each Au wire serves to induce a proximity effect⁵. With this design, simple heat flow simulations show that the temperature profile across the thermometer is essentially flat¹⁰. At one end of the Andreev interferometer, a heater is formed from a wide Au strip that is in direct electrical contact with the Andreev interferometer and one thermometer (the ‘hot’ thermometer). Two other thermometers measure the temperature at the other end of the Andreev interferometer (the ‘cold’ thermometers, only one is used). By passing a dc current through the heater, one can heat one end of the Andreev interferometer to a temperature above the substrate temperature T_b . Electrical contact to the heater and all thermometers is made through superconductors whose thermal conduction is small, so that at temperatures below approximately half the critical temperature T_c of the Al, the power P generated in the heater can flow out essentially only through the Andreev interferometer. (The electron-phonon scattering rate is at least three orders of magnitude smaller than the electron-electron scattering rate at these temperatures¹¹, so that heat flow through the phonons is much smaller than the electronic conduction through the interferometer, and is ignored in our analysis.) The normal metal parts of the heater, thermometers, and the Andreev interferometer itself are fabricated at the same time, so that the coupling of the electrons in the thermometer with the electrons in the heater and samples is very good. By measuring the voltage drop across the heater, and knowing the current through it, we therefore have a quantitative estimate of the heat flow $I^T = P$ through the Andreev interferometer.

The thermometers are first calibrated by measuring their four-terminal resistance with an ac resistance bridge with no current in the heater as a function of the temperature of the cryostat, which in this experiment was a ^3He sorption refrigerator with a base temperature of 260 mK. The temperature of the refrigerator is then kept fixed, and the ac resistance of the thermometers is measured as a function of dc current through the heater. By cross-correlation of the two measurements, one can obtain the temperature of the electrons in the thermometers as a function of the power through the heater. Fig. 2(a) shows the result of these measurements for the hot and cold thermometer. At low heater power ($\leq 10 \text{ pW}$), only the hot thermometer shows a change in temperature, while at higher heater powers, both thermometers show an increase in electron temperature. We also show in the same figure the difference in temperature ΔT as a function of heater power, which grows as expected.

The thermal conductance of the Andreev interferometer can now be essentially read directly from Fig. 2(a), since it is given by $G^T = P/\Delta T$. Fig. 2(b) shows a plot of $P/\Delta T$ as a function of the average temperature. Ideally, one should measure the thermal conductance in the limit of $\Delta T \rightarrow 0$. This limit can be obtained by extrapolating the curve in Fig. 2(b) to the case when $T_{ave} = (T_h + T_c)/2$ approaches base temperature, in the limit of zero power

through the heater. Performing this extrapolation, one obtains a conductance of $G^T = 1.2 \times 10^{-10}$ W/K.

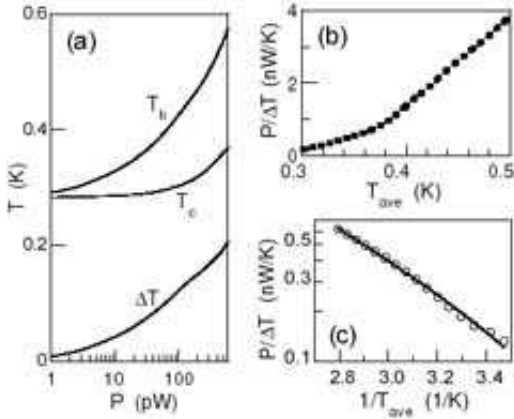


FIG. 2. (a) Temperature of hot and cold thermometers and their difference as a function of power dissipation in the heater at $T_b = 280$ mK. (b) Thermal conductance as a function of the average temperature $T_{ave} = (T_h + T_c)/2$ of the Andreev interferometer. (c) Low power regime in a semi-logarithmic plot, demonstrating the exponential dependence of the conductance on inverse temperature. Solid line is a fit to the expected dependence for a superconductor.

In order to put this number in context, it is instructive to calculate the thermal conductance of a gold wire of the same dimensions as in the Andreev interferometer, but without the superconductor. This can be estimated from the Wiedemann-Franz law³, which states that the ratio of the thermal to the electrical conductivity of a metal is proportional to the temperature. In terms of conductances, one can write this as $G^T = AT/R$, where the textbook value³ of the constant A for Au is 2.32×10^{-8} WΩ/K². With this value for A , and the measured value of the normal state resistance R , we can estimate the thermal conductance of the equivalent Au wire to be 1.3×10^{-9} W/K, more than an order of magnitude higher than the measured thermal conductance of the Andreev interferometer.

Although small deviations from the Wiedemann-Franz law are expected for real metals, the order of magnitude difference suggests that the superconductor present in the Andreev interferometer has a substantial effect on its thermal conductance. A reasonable first approximation is to estimate the thermal conductance of the small section of the proximity coupled normal part of Andreev interferometer (between the superconducting arms) as a superconductor. The thermal conductance of a superconductor arises solely from the presence of quasiparticles in the superconductor, whose population is exponentially suppressed at temperatures well below the superconducting gap. Consequently, the thermal conductance of a superconductor at low temperatures is given by an equation of the form¹²

$$G_S^T \approx G_N^T \cdot \frac{6}{\pi^2} \left(\frac{\Delta}{k_B T} \right)^2 e^{-\Delta/k_B T}, \quad (3)$$

where G_N^T is the thermal conductance in the normal state, and Δ is the superconducting gap. Fig. 2(c) shows a plot of an expanded version of the low power regime of G_S^T as a function of the inverse average temperature, along with a fit to the equation above. From this, we obtain a gap $\Delta = 200$ μeV, which compares favorably with the value $\Delta = 183$ μeV obtained from the measured T_c of the Al.

As we noted earlier, the electrical conductance and thermopower of such Andreev interferometers are expected to oscillate as a function of applied magnetic flux with a fundamental period $h/2e$, due to the quantum interference of quasiparticles in the proximity coupled normal metal⁵. With the local thermometers we can now obtain *quantitative* measurements of the thermopower oscillations. The thermal voltage across the Andreev interferometer is given by

$$\Delta V = \int_{T_c}^{T_h(I)} S_A dT, \quad (4)$$

where S_A is the thermopower of the interferometer. We have ignored here the thermopower contribution of the V_+ voltage contact (see Fig. 1(a)), which is acceptable if it is small, or does not vary as a function of external parameters (as is the case in our experiments). In order to improve our sensitivity, we use an ac technique⁹ by superposing an ac tickling current on top of the dc heater current, which implies that we measure the derivative

$$\frac{d(\Delta V)}{dI} = S_A \frac{dT_h}{dI}, \quad (5)$$

where we have assumed that we are in the low current regime in Fig. 2(a) (≤ 10 μW), so that the temperature of the cold thermometer is constant ($dT_c/dI = 0$). dT_h/dI can be numerically obtained from $T_h(I)$, so that a quantitative estimate of the thermopower can be directly obtained from the measured ac voltage.

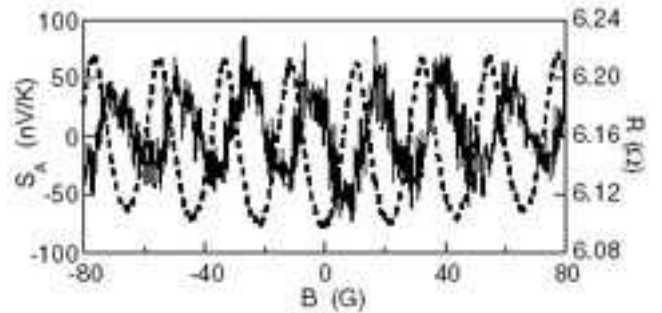


FIG. 3. Magnetic flux dependence of the resistance (dashed curve) and thermopower (solid curve) of the Andreev interferometer at $T_b = 295$ mK.

Fig. 3 shows the thermopower S_A and the resistance R of the Andreev interferometer as a function of the applied magnetic field B . The thermopower data were taken with a dc current of $5\ \mu\text{A}$ and an ac current of rms amplitude $1\ \mu\text{A}$ through the heater. Both quantities oscillate as a function of B with a fundamental period corresponding to a flux $h/2e$ through the area of the interferometer. However, while the oscillations in R are symmetric in B , the oscillations in S_A are antisymmetric. A negative thermopower in a metal is typically associated with electron-like charge carriers, while a positive thermopower is associated with hole-like charge carriers. An antisymmetric S_A means that the modulation of the quantum interference in the Andreev interferometer by the magnetic field periodically changes the sign of the thermopower in the interferometer.

Two aspects of our results are worthy of note. First, at the level of our measurement sensitivity, the thermal conductance of the Andreev interferometer does not oscillate with B , although one might expect such oscillations based on the fact that R and S oscillate with B^5 . Unlike the electrical properties, however, the thermal conductance of the Andreev interferometer is determined by the series addition of the thermal conductance of the proximity coupled normal-metal wires, and the small section of the superconductor which lies across the normal metal. Since the thermal conductance of this last section of the superconductor is about an order of magnitude smaller than that of the normal metal regions, it determines the thermal conductance of the entire sample. Consequently, the small variations of the thermal conductance in the normal metal regions associated with the proximity effect will not be observable. Second, the symmetry of the thermopower with respect to magnetic field is similar to what has been observed earlier⁹, where it was noted that this symmetry (symmetric or antisymmetric with respect to field) appeared to depend on sample geometry. The origin of this behavior is still not understood. The measurements reported here confirm the results of the earlier experiments, and may also provide a possible clue to the origin of the dependence of the symmetry on sample topology. For Andreev interferometers where the superconductor lies in the path of the heat current, the low thermal conductivity of the superconductor implies that essentially all the temperature differential is dropped

across it, and none across the proximity coupled normal metal, so that no thermal voltage is developed across the normal metal (the superconductor, of course, has no thermal voltage). For Andreev interferometers where the superconductor is not in the path of the heat current, one would have a large contribution to the thermopower from the proximity coupled normal metal. While this does not explain the symmetry of the thermopower with respect to magnetic field, it does indicate why one might expect zero thermopower contribution in the absence of a magnetic field for Andreev interferometers of the first type, as is observed. Further work is required to fully understand the magnetic field dependence.

This work was supported by the NSF through DMR-9801982, and by the David and Lucile Packard Foundation.

-
- ¹ K. Schwab, E.A. Henriksen, J.M. Worlock and M.L. Roukes, *Nature* **404**, 974 (2000).
 - ² J. Aumentado, V. Chandrasekhar, J. Eom, P.M. Baldo and L.E. Rehn, *Appl. Phys. Lett.* **75**, 3554 (1999).
 - ³ N.W. Ashcroft, N.D. Mermin, *Solid State Physics*, [Saunders College Publishing, Orlando, 1976].
 - ⁴ H. Pothier, S. Gueron, N.O. Birge, D. Esteve and M.H. Devoret, *Phys. Rev. Lett.* **79**, 3490 (1997).
 - ⁵ For a recent review, see W. Belzig *et al.*, *Superlatt. Microstruct.* **25**, 1251 (1999).
 - ⁶ P. Mohanty, E.M.Q. Jariwala and R.A. Webb, *Phys. Rev. Lett.* **78**, 3366 (1997) and references there.
 - ⁷ H. Nakano, H. Takayanagi, *Solid State Comm.* **80**, 997 (1991).
 - ⁸ H. Pothier, S. Gueron, D. Esteve and M.H. Devoret, *Phys. Rev. Lett.* **73**, 2488 (1994).
 - ⁹ J. Eom, C.-J. Chien and V. Chandrasekhar, *Phys. Rev. Lett.* **81**, 437 (1998).
 - ¹⁰ K.E. Nagaev, *Phys. Rev. B* **52**, 4740 (1995).
 - ¹¹ S. Wind, M.J. Rooks, V. Chandrasekhar and D.E. Prober, *Phys. Rev. Lett.* **57**, 633 (1986).
 - ¹² A.A. Abrikosov, *Fundamentals of the theory of metals*, [Elsevier Science Pub. Co., Amsterdam, 1988].